PHYSICS AND CHEMISTRY
OF SOLID STATE
V. 21, No. 4 (2020) pp. 720-726

DOI: 10.15330/pcss.21.4.720-726

Vasyl Stefanyk Precarpathian
National University

ФІЗИКА І ХІМІЯ ТВЕРДОГО ТІЛА
Т. 21, № 4 (2020) С. 720-726

PACS: 61.72.Cc, 64.75.Op, 66.30.Dn, 66.30.Ny, 66.30.Pa, 68.35.Fx, 68.35.Rh ISSN 1729-4428

M.V. Yarmolenko

Intrinsic Diffusivities Ratio Analysis in the Al-Cu System

Kyiv National University of Technologies and Design, Faculty of Market, Information and Innovation Technologies, Cherkasy, Ukraine; yarmolenko.mv@knutd.edu.ua

Copper and aluminium electric corrosion rates are investigated experimentally at room temperature and at temperature 100 ºC. It is founded that copper corrosion is higher than aluminium corrosion, and ratio of electric corrosion rates, k_{Cu}/k_{Al} , decreases with temperature increasing. It is calculated that copper corrosion rate is approximately equal to aluminium corrosion at temperature about 300 ºC due to Cu^{2+} ions are less mobile than Cu^{+} ions. It is obvious physically: the higher temperature is, the grater atoms' displacements in crystal lattice, Cu atoms can diffuse without two electrons, and Cu^{2+} ions more strongly interact with crystal lattice than Cu^{+} ions. Literature data analysis shows than Cu rich intermetallic compounds (IMCs) are formed faster in Cu-Al system at temperature lower than 400 ºC, and the Kirkendall plane shifts toward Cu side, but Al rich IMCs are formed faster in Cu-Al system at temperature higher than 475 ºC, and the Kirkendall plane shifts toward Al side. It is concluded that Cu^{2+} ions diffuse in IMCs at temperature higher than 475 ºC, but Cu^{+} ions diffuse in IMCs at temperature lower than 400ºC. A theoretical method to calculate intrinsic diffusivities ratio in double multiphase systems is proposed. The method involves the Kirkendall plane displacement and the general phases thickness only. Intrinsic diffusivities ratios in the Al-Cu system are calculated using literature experimental data. Diffusion activation energies and pre-exponential coefficients for the Cu-Al system are calculated combining literature experimental results. Analysis of literature data shows that the Kirkendall shift changes sign at temperature about 460ºC in the Cu-Al system because of intrinsic diffusivities ratio, D_{Cu}^*/D_{Al}^*, dependence from temperature. Such result agrees with copper and aluminium electric corrosion rates investigation.

Key words: diffusion, intermetallic compounds, phases formation kinetics, copper, aluminium, the Kirkendall-Frenkel porosity, the Kirkendall shift.

Received 26 November 2020; Accepted 15 December 2020.

Introduction

The Cu-clad Al (CA) wire, where the CA wire is an Al wire coated with Cu (≈ 15µm thickness), is widely used for electronic parts as a conductive material in the automobile industry. The CA wire utilized near the motor in the automobile is heated at temperatures of about 373-473 K (100 - 200°C). Intermetallics can formed at the Cu/Al interface and grow gradually during heating at such temperatures. The IMC layers are brittle and electrically resistant. As a consequence, the growths of the IMC layers deteriorate mechanical and electrical properties of the CA wire. Therefore, for assurance of the reliability of the product, information on the growth behaviour of the IMC layers during heating is essentially important [1].

Otherwise, it was proved experimentally that thin Al pad (≈ 1 µm thickness) can prevent gold and copper corrosion, because intermetallics formation rate in Au-Al system is much more higher than intermetallics formation rate in Cu-Al system, so it is possible to use Cu instead of Au for wire bonding in microelectronics packaging, and Cu has higher electric conductivity, higher thermal conduction, and lower material cost than Au [2]. It was founded experimentally, that copper electric corrosion is higher than aluminium electric corrosion in approximately two times at temperatures less than 40 ºC [3, 4], so thin Al layer can prevent copper electric corrosion.

Besides, one of the most common reasons for chip failure is due to the soldered copper/tin based contacts, that is, the soldered contacts are the weakest part of the chip and this is related, in particular, to intermetallics and the Kirkendall-Frenkel porosity formation in the contact

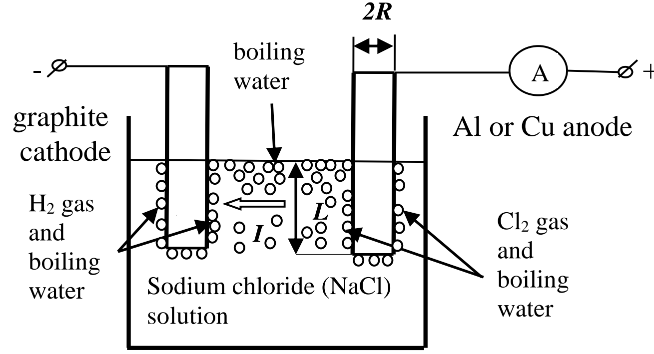

Fig. 1. Scheme of experimental equipment ($T = 100\ ^oC$).

zone [5]. The temperature range is from room temperature up to 250°C (typical range of packaging and operation of the integrated circuits) [6, 7].

Hydrostatic pressure of Argon gas (≈ 10 MPa) can decrease Kirkendal-Frenkel porosity formation, but practically can't decrease mutual diffusion coefficients [8]. Hot isostatic pressing (p ≈ 100 MPa, Argon) removes porosity due to homogenisation heat treatment in alloy CMSX4 and superalloy CMSX10 [9].

Electric current can destruct wire bonding in microelectronics packaging, so we planned to investigate copper and aluminium electric corrosion at room temperature and at temperature 100 ºC. Direct current can dissolve metal anode into electrolyte, and we planned to do experiments under the same conditions: initial radii of Al and Cu anodes should be approximately equal, electrolyte concentration should be the same, anodes lengths immersed into electrolyte should be equal, graphite cathodes should be the same, direct electric current value should be practically the same.

I. Experimental results of copper and aluminium electric corrosion investigation at temperature 100 ºC

Experiments were carried at room temperature [3, 4] and at temperature 100 ºC. Cylindrical anodes (99.99 % Cu and 99.99 % Al) were used for copper and aluminium electric corrosion investigation. Sodium chloride (NaCl) solution was used as electrolyte (Fig. 1).

Direct electric current and anodes mass decreasing were measured. Rate of anode dissolving into electrolyte can be calculated using Faraday's law of electrolysis:

$$\frac{dm}{dt} = \frac{MI}{zF}, \quad dm = \rho \cdot L \cdot \pi \cdot d(R^2(t)), \tag{1}$$

where m is the anode mass dissolved into the electrolyte, t is the time of experiment, M is the molar mass, I is the direct electric current value, F is the Faraday constant ($F \approx 96500\ C\ mol^{-1}$), z is the charge of ions, R is the anode radius, L is the anode length immersed into the electrolyte.

Electric current value did not change, so one can calculate:

$$z = \frac{MIt}{F\pi\rho L(R^2(t=0) - R^2(t))}, \tag{2}$$

where ρ is the anode density. Charges of copper and aluminium ions were calculated:

$$z_{Cu} = \frac{63.55 \cdot 10^{-3}\, kg/mol \cdot 3.05A \cdot 1.2 \cdot 10^3 s}{F \cdot \pi \cdot 8.9 \cdot 10^3\, kg/m^3\, L_{Cu} \cdot (R^2_{Cu}(t=0) - R^2_{Cu}(t_4))} \approx 1.47 \approx \frac{1+2}{2}, \tag{3}$$

$$z_{Al} = \frac{27 \cdot 10^{-3}\, kg/mol \cdot 3.15A \cdot 1.2 \cdot 10^3 s}{F \cdot \pi \cdot 2.7 \cdot 10^3\, kg/m^3\, L_{Al} \cdot (R^2_{Al}(t=0) - R^2_{Al}(t_4))} \approx 2.85 \approx 3, \tag{4}$$

where $L_{Cu} = L_{Al} = 4 \cdot 10^{-2}$ m, $R_{0Cu} = 2.27$ mm, $R_{0Al} = 2.6$ mm, $I_{Al} = 3.15$ A, $I_{Cu} = 3.05$ A, so copper dissolved into NaCl solution as Cu^+ and Cu^{2+} ions (copper dissolved into NaCl solution as Cu^+ ions at room temperature), and aluminium dissolved into NaCl solution as Al^{3+} ions. Anodes radii decreasing kinetics is shown on Fig. 2.

Experiments were carried during $t_1 = 5$ *min*, $t_2 = 10$ *min*, $t_3 = 15$ *min, and* $t_4 = 20$ *min*. Experimental results are as follows: $R_{1Cu} = 2.2$ *mm*, $R_{2Cu} = 2.12$ *mm*, $R_{3Cu} = 2.03$ *mm*, $R_{4Cu} = 1.92$ *mm*; $R_{1Al} = 2.56$ *mm*, $R_{2Al} = 2.51$ *mm*, $R_{3Al} = 2.45$ *mm*, $R_{4Al} = 2.38$ *mm*. Measurement precision was *0.01 mm* or *10 micrometer*. We carried additional experiments, but result was the same.

Chemical reactions are more complicated at 100°C than at room temperature [3, 4] near positive electrodes (anodes):

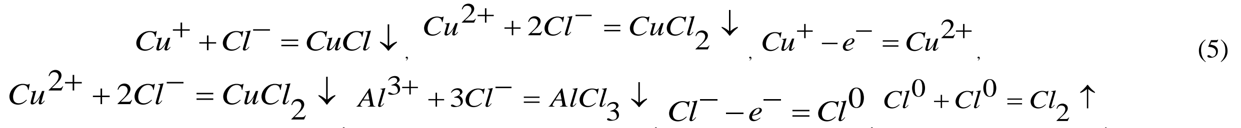

$$Cu^{+} + Cl^{-} = CuCl\downarrow,\quad Cu^{2+} + 2Cl^{-} = CuCl_2\downarrow,\quad Cu^{+} - e^{-} = Cu^{2+},$$
$$Cu^{2+} + 2Cl^{-} = CuCl_2\downarrow,\quad Al^{3+} + 3Cl^{-} = AlCl_3\downarrow,\quad Cl^{-} - e^{-} = Cl^{0},\quad Cl^{0} + Cl^{0} = Cl_2\uparrow. \tag{5}$$

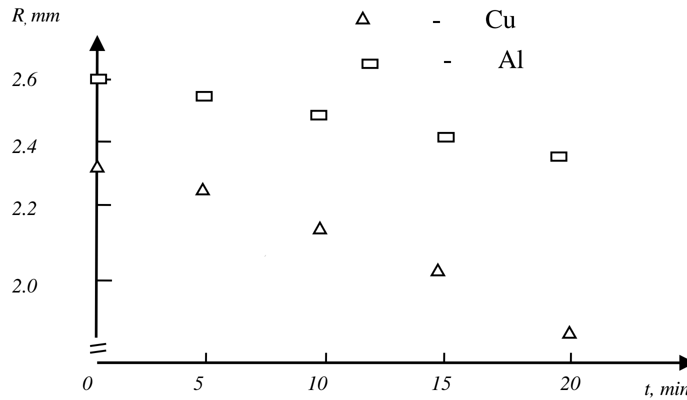

Fig. 2. Al and Cu anodes radii decreasing kinetics at $T = 100\,^oC$.

Chlorine gas and boiling water were formed near anodes.

Chemical reactions took place near negative electrodes (cathodes):

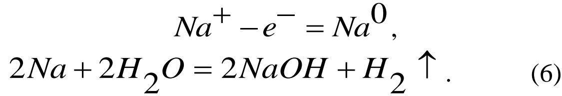

$$Na^{+} - e^{-} = Na^{0},$$
$$2Na + 2H_2O = 2NaOH + H_2\uparrow. \tag{6}$$

Hydrogen gas and boiling water were formed near cathodes.

Anodes radii decreasing rate constants can be calculated as average value of four experiments:

$$k_{Cu} = \frac{4R_0^2 - \sum_{i=1}^{4} R_i^2}{\sum_{i=1}^{4} t_i} \approx 1.154\cdot 10^{-9} m^2/s, \tag{7}$$

{1.25 at room temperature},

$$k_{Al} = \frac{4R_0^2 - \sum_{i=1}^{4} R_i^2}{\sum_{i=1}^{4} t_i} \approx 8.42\cdot 10^{-10} m^2/s,$$

{7.29 at room temperature},

$$k_{Cu} \approx 1.37 k_{Al}, \{1.72 \text{ at room temperature } T_1 = 27^oC\}, \tag{8}$$

so copper electric corrosion is higher at room temperature $T_1 = 27^oC$, aluminium electric corrosion is higher at temperature $T_2 = 100^oC$, and ratio of electric corrosion rates, k_{Cu}/k_{Al} , decreases with temperature increasing. We can conclude that Cu^{2+} ions are less mobile than Cu^{+} ions. It is need to point out that k_{Cu} and k_{Al} have dimensionalities as diffusion coefficients, m^2/s, because of the anodes cylindrical shape. Such result allows us to calculate:

$$\frac{k_{Cu}}{k_{Al}}(T) \approx \frac{D^*_{Cu}}{D^*_{Al}}(T) = \frac{D^*_{0Cu}}{D^*_{0Al}} e^{(Q_{Al}-Q_{Cu})/(RT)}; \ln\left(\frac{D^*_{0Cu}}{D^*_{0Al}}\right) = -0.6; Q_{Al} - Q_{Cu} = 2.9 kJ/mol, \tag{9}$$

$$\frac{D^*_{0Cu}}{D^*_{0Al}} = 0.55, \quad \frac{D^*_{Cu}}{D^*_{Al}}(T_3) = 1 \Rightarrow T_3 = \frac{2900 J/mol}{0.6R} \approx 583K \approx 310^o C, \tag{10}$$

so $Q_{Al} > Q_{Cu}$ because Cu^{+} ions have higher mobilities than Al^{3+} ions.

II. Method

The Kirkendall shift , X_K, can be calculated in such a way [10]:

$$X_K^2 = \frac{4(\sqrt{D_B^*} - \sqrt{D_A^*})^2}{\pi} t = \left(1 - \sqrt{\frac{D_A^*}{D_B^*}}\right)^2 \frac{4D_B^*}{\pi} t, \quad \frac{D_B^*}{D_A^*} > 1, \quad (11)$$

or [11]:

$$X_K^2 = \frac{2(D_B^* - D_A^*)^2}{\pi(D_B^* + D_A^*)} t = \frac{\left(1 - D_A^*/D_B^*\right)^2}{1 + D_A^*/D_B^*} \frac{2D_B^*}{\pi} t, \quad \frac{D_B^*}{D_A^*} > 1, \quad (12)$$

or [12]:

$$X_K^2 = \frac{(D_B^* - D_A^*)^2}{\pi D_B^*} t = \left(1 - \frac{D_A^*}{D_B^*}\right)^2 \frac{D_B^*}{\pi} t, \quad \frac{D_B^*}{D_A^*} > 1 \quad (13)$$

Eqs. 11, 12, and 13 give exactly the same result in the case $D_B^* \approx D_A^*$ and slightly different results (on approximately 15 percents) in the case $D_B^* \approx 2D_A^*$.

Intrinsic diffusivities ratio D^*_A/D^*_B can be calculated using Darken's method [13]:

$$D^*_I = C_i D^*_A + (1-C_i) D^*_B = D_i/\Delta C_i, \quad C_i = C_B, \quad (14)$$

$$\frac{D_A^*}{D_B^*} = \frac{\sqrt{D_i^* t} - X_K(1 - C_i)\sqrt{\pi}}{\sqrt{D_i^* t} + C_i X_K \sqrt{\pi}} < 1, \quad (15)$$

where D_i^* is the mutual diffusion coefficient in phase i, $D_i = D_i^* \Delta C_i$ is the mutual diffusion penetrability in phase i, C_i is the average concentration of substance B in phase i, ΔC_i is phase i's homogeneity range. It was experimentally obtained [8] that $\sqrt{D_i^* t}$ is approximately equal to general diffusion zone width, so we can get finally:

$$\frac{D_A^*}{D_B^*} \approx \frac{\sum_{j=1}^{N} X_j - X_K(1 - C_i)\sqrt{\pi}}{\sum_{j=1}^{N} X_j + C_i X_K \sqrt{\pi}} < 1 \quad C_i = C_B, \quad (16)$$

where N is formed phases quantity, X_j is phase j's thickness, C_i is is the average concentration of substance B in phase i.

III. Analysis for the Al-Cu system

Five phases are formed in Al-Cu system at temperatures from 400 ºC to 535 ºC [14] and at temperatures from 210 ºC to 270 ºC [1]: θ-phase (phase 1) $CuAl_2$ ($C_1 = 2/3$), η_2-phase (phase 2) CuAl ($C_2 = 1/2$), ζ_2-phase (phase 3b) Cu_4Al_3 ($C_{3b} = 3/7$), δ-phase (phase 3a) Cu_3Al_2 ($C_{3a} = 2/5$), and γ_2-phase (phase 3) Cu_9Al_4 ($C_3 = 4/13 \approx 0.31 \approx 1/3$, $C = C_{Al}$). Authors obtained [14]:

$$\tilde{D}_1^* = 5.6x10^{-5} e^{-127.6kJmol^{-1}/(RT)} m^2/s; \quad \tilde{D}_2^* = 2.2x10^{-4} e^{-148.5kJmol^{-1}/(RT)} m^2/s;$$
$$\tilde{D}_{3b}^* = 1.6x10^{2} e^{-230.5kJmol^{-1}/(RT)} m^2/s; \quad \tilde{D}_{3a}^* = 2.1x10^{-4} e^{-138.1kJmol^{-1}/(RT)} m^2/s; \quad (17)$$
$$\tilde{D}_3^* = 8.5x10^{-5} e^{-136kJmol^{-1}/(RT)} m^2/s.$$

We can see that $Q_1 < Q_2$, $Q_1 < Q_3$, and $Q_3 < Q_2$ because of $K_1 > K_2$, $K_1 > K_3$, $K_3 > K_2$, and $D_{01} \approx D_{02} \approx D_{03}$. Phase j's rate formation is K_j. We are interested in intermetallics disappearance rate analysis, so we can consider phases Cu_4Al_3 (phase 3b), Cu_3Al_2 (phase 3a), and Cu_9Al_4 as one "phase 3" with average Al concentration $C_3 \approx 1/3$. Authors [1] considered phases 2, 3b, 3a, and 3 as "phase 2" [1]. Three phases are formed in Al-Cu system at temperatures from 175ºC to 225 ºC [2] and at temperatures from 300ºC to 400 ºC [15]: $CuAl_2$, CuAl, and Cu_9Al_4. Some experimental results are listed in Table 1, so $X_1 > X_2$, $X_1 > X_3$, but $X_2 < X_3$, because of, maybe, high ordered phase CuAl (body-centered orthorhombic crystal structure) like phase

Table 1

Phases 1, 2, and 3 formation rates comparison in Al-Cu system

Authors	*T, ºC*	*t, h*	K_1, $x10^{-18}$ m^2/s	K_2, $x10^{-18}$ m^2/s	K_3, $x10^{-18}$ m^2/s	K_{123}, $x10^{-18}$ m^2/s	K_1/K_2	K_1/K_3	K_3/K_2	K_{123}/K_3
1.Funamizu and Watanabe [14]	*515*	*40*	6990	630	K_{3b}= 3030	K_{123b}= 26730	11.1	2.3	4.8	8.9
2.Gueydan *et al.*[15]	400	24	1400	300	760	6800	4.7	1.8	2.5	8.9
3.Moisy *et al.*[16]	350	2	860	100	370	3400	8.6	2.3	3.7	9.2
4.Moisy *et al.* [16]	300	2	77	18	55	420	4.3	1.4	3.1	7.6
5.Goh *et al.*[2]	225	480	-	-	-	0.715		-	-	-

CuZn. It was reported that diffusivity of Cu is higher than diffusivity of Al at temperatures 300ºC ÷ 350ºC [16].

We can use Eq. 14 to calculate mutual diffusion coefficients in each phase at temperature 100ºC:

$$D_1 = C_1 D_{Cu} + (1-C_1)D_{Al} = (\frac{2}{3}\cdot 1.37 + \frac{1}{3})D_{Al} \approx 1.25 D_{Al},$$
$$D_2 = C_2 D_{Cu} + (1-C_2)D_{Al} = \left(\frac{1}{2}\cdot 1.37 + \frac{1}{2}\right)D_{Al} \approx 1.19 D_{Al}, \quad (18)$$
$$D_3 = C_3 D_{Cu} + (1-C_3)D_{Al} = (\frac{1}{3}\cdot 1.37 + \frac{2}{3})D_{Al} \approx 1.12 D_{Al},$$

so $X_1 \approx \sqrt{\frac{D_1}{D_3}} X_3 \approx 1.06 X_3$, $X_2 \approx \sqrt{\frac{D_2}{D_3}} X_3 \approx 1.03 X_3$, $X_1 \geq X_2 \geq X_3$, and Al rich phases are formed more quickly, because Al-atoms and Cu-atoms move in opposite directions, vacancies can disappear near dislocations at Cu side (sinks) and appear near dislocations at Al side (sources), dislocations can climb ([17], Fig.6.24), and Kirkendall plane shifts toward Cu side.

Otherwise, it was reported that diffusivity of Al is higher than diffusivity of Cu at temperatures 475 ºC ÷ 535 ºC, and the markers moves toward Al side [14].

Authors [14] didn't calculate ratio D^*_{Al}/D^*_{Cu}. We can analyse described experimental results in Al-Cu system ($T_2 = 515^oC = 788\ K$, $t = 40h$, $X_K \approx 11\mu m$, $X_1 + X_2 + X_{3b} + X_{3a} + X_3 \approx 127\ \mu m$):

$$\frac{D^*_{Cu}}{D^*_{Al}}(T_2 = 515^o C) \approx \frac{X_1 + X_2 + X_{3b} + X_{3a} + X_3 - X_K(1-C_2)\sqrt{\pi}}{X_1 + X_2 + X_{3b} + X_{3a} + X_3 + C_2 X_K\sqrt{\pi}} \approx 0.856;\ y_2 = \frac{D^*_{Al}}{D^*_{Cu}} = 1.168\cdot \quad (19)$$

Markers were in phase 3b (ζ_2-phase Cu_4Al_3, monoclinic crystal structure). Cu_3Al_2 phase has γ-brass type crystal structure, a = 8.70 Å, like phase 3, Cu_9Al_4, a = 8.69 Å [14]. Phases 3, 3a and 3b are very similar, so it is difficult to identify them by SEM and EDS [1]. Ratio D^*_{Al}/D^*_{Cu} depends on temperature ($T_4 = 475\ ^oC = 748\ K$, $t = 90\ h$, $X_K \approx 2\mu m$, $X_1 + X_2 + X_{3b} + X_{3a} + X_3 \approx 113\mu m$):

$$\frac{D^*_{Cu}}{D^*_{Al}}(T_4 = 475^o C) \approx \frac{X_1 + X_2 + X_{3b} + X_{3a} + X_3 - X_K(1-0.4)\sqrt{\pi}}{X_1 + X_2 + X_{3b} + X_{3a} + X_3 + 0.4CX_K\sqrt{\pi}} \approx 0.969;\ y_4 = \frac{D^*_{Al}}{D^*_{Cu}} = 1.032\cdot \quad (20)$$

We can find additional two points ($T_1 = 535\ ^oC = 808\ K$, $t = 40\ h$, $X_K \approx 20.5\ \mu m$, $X_1 + X_2 + X_{3b} + X_{3a} + X_3 \approx 180\mu m$; $T_3 = 495\ ^oC = 768\ K$, $t = 40\ h$, $X_K \approx 5\ \mu m$, $X_1 + X_2 + X_{3b} + X_{3a} + X_3 \approx 101\mu m,$):

$$\frac{D^*_{Cu}}{D^*_{Al}}(T_1 = 535^o C) \approx \frac{X_1 + X_2 + X_{3b} + X_{3a} + X_3 - X_K 0.6\sqrt{\pi}}{X_1 + X_2 + X_{3b} + X_{3a} + X_3 + 0.4X_K\sqrt{\pi}} \approx 0.814;\ y_1 = 1.228\cdot \quad (21)$$

$$\frac{D^*_{Cu}}{D^*_{Al}}(T_3 = 495^o C) \approx \frac{X_1 + X_2 + X_{3b} + X_{3a} + X_3 - X_K 0.6\sqrt{\pi}}{X_1 + X_2 + X_{3b} + X_{3a} + X_3 + 0.4X_K\sqrt{\pi}} \approx 0.916;\ y_3 = 1.092\cdot \quad (22)$$

We can use these four points to calculate by the least square method:

$$\Delta Q = Q_{Al} - Q_{Cu} = \frac{4\sum_{j=1}^{4}\left(\frac{1000}{RT_j}\ln y_j\right) - \sum_{j=1}^{4}\ln y_j \sum_{j=1}^{4}\frac{1000}{RT_j}}{4\sum_{j=1}^{4}\left(\frac{1000}{RT_j}\right)^2 - \left(\sum_{j=1}^{4}\frac{1000}{RT_j}\right)^2} \approx -13.4 kJ/mol, \quad (23)$$

$$y_0 = \exp\frac{\sum_{j=1}^{4}\left(\frac{1000}{RT_j}\right)^2\sum_{j=1}^{4}\ln y_j - \sum_{j=1}^{4}\frac{1000}{RT_j}\sum_{j=1}^{4}\left(\frac{1000}{RT_j}\ln y_j\right)}{4\sum_{j=1}^{4}\left(\frac{1000}{RT_j}\right)^2 - \left(\sum_{j=1}^{4}\frac{1000}{RT_j}\right)^2} \approx \exp(2.2) \approx 9, \quad (24)$$

$$\frac{D^*_{Al}}{D^*_{Cu}}(T) = \frac{D^*_{0Al}}{D^*_{0Cu}} e^{(Q_{Al}-Q_{Cu})/(RT)} \approx 9e^{-13.4kJ/mol/(RT)}, \quad (25)$$

$$\frac{D^*_{Al}}{D^*_{Cu}}(T_5) = y_5 = 1 \Rightarrow T_5 = \frac{13400J/mol}{R\ln 9} \approx 733K \approx 460^{O}C, \quad (26)$$

So $Q_{AL}<Q_{CU}$ because CU^{2+} ions have less mobilities than al^{3+} ions, and we can conclude that the kirkendall shift changes sign at temperature about $460^{O}C$.

IV. Diffusion activation energy calculation in the Cu-Al system

Authors [16] didn't calculate diffusion activation energies and the pre-exponential factors, so we can do it using calculated data by k. p. gurov's and a. m. gusak's method or "constant flux method" [3,4,18-23] (Table 2) and eqs. 27:

$$Q_i = \frac{RT_1T_2}{T_2-T_1}\ln\left(\frac{D_i(T_2)}{D_i(T_1)}\right),$$
$$D_{0i} = D_i(T_1)e^{Q_i/(RT_1)} = D_i(T_2)e^{Q_i/(RT_2)} \quad (27)$$

$$\tilde{D}_1 = 4.3x10^{-5}e^{-136.7kJmol^{-1}/(RT)}m^2/s;$$
$$\tilde{D}_2 = 6.6x10^{-8}e^{-108.8kJmol^{-1}/(RT)}m^2/s; \quad (28)$$
$$\tilde{D}_3 = 9.6x10^{-7}e^{-119.6kJmol^{-1}/(RT)}m^2/s.$$

Equations 28 correspond to obtained results [14] (eQS.17). it should be $Q_1 < Q_2$, $Q_1 < Q_3$, and $Q_3 < Q_2$ because of $K_1 > K_2$, $K_1 > K_3$, and $K_3 > K_2$ if $D_{01} \approx D_{02} \approx D_{03}$ [14].

Conclusions

Copper corrosion is higher than aluminium corrosion, and ratio of electric corrosion rates, k_{Cu}/k_{Al}, decreases with temperature increasing. Copper corrosion rate is approximately equal to aluminium corrosion at temperature about 300 °C due to Cu^{2+} ions are less mobile than Cu^{+} ions. It is obvious physically: the higher temperature is, the grater atoms' displacements in crystal lattice, Cu atoms can diffuse without two electrons, and Cu^{2+} ions more strongly interact with crystal lattice than Cu^{+} ions.

Cu rich intermetallic compounds (IMCs) are formed faster in Cu-Al system at temperature lower than 400 °C, and the Kirkendall plane shifts toward Cu side, but Al rich IMCs are formed faster in Cu-Al system at temperature higher than 475 °C, and the Kirkendall plane shifts toward Al side. Cu^{2+} ions diffuse in IMCs at temperature higher than 475 °C, but Cu^{+} ions diffuse in IMCs at temperature lower than 400 °C.

Diffusion activation energy of Al is less than diffusion activation energy of Cu at temperature higher than 475°C and Cu^{2+} ions have less mobilities than Al^{3+}.

The Kirkendall shift changes sign at temperature about 460 °C in the Cu-Al system because of intrinsic diffusivities ratio, D_{Cu}^*/D_{Al}^*, dependence from temperature. Such result agrees with copper and aluminium electric corrosion rates investigation.

Table 2

Diffusion penetrabilities calculated using "constant flux method" in Al-Cu system (authors' method [14] is grounded on Heumann's method, and we assume $\Delta C_1 \approx \Delta C_2 \approx \Delta C_3 \approx 0.01$).

Authors	T, °C	t, h	D_1, $x10^{-18}$ m^2/s	D_2, $x10^{-18}$ m^2/s	D_3, $x10^{-18}$ m^2/s
Funamizu and Watanabe [14]	515	40	1800	300	800
This work	515	-	1300	400	1140
Gueydan *et al.* [15]	400	24	-	-	-
This work	400	-	270	130	180
Moisy *et al.* [16]	350	2	-	-	-
This work	350	-	150	50	90
Moisy *et al.* [16]	300	2	-	-	-
This work	300	-	15	8	12

Yarmolenko M.V. - Ph.D., Associate Professor, Head of the Department of Information and Computer Technologies and Fundamental Disciplines.

[1] T. Kizaki, M.O, and M. Kajihara, Materials Transactions 61(1), 188 (2020) (https://10.2320/matertrans.MT-M2019207).
[2] C.S. Goh, W.L.E. Chong, T.K. Lee, and C. Breach, Crystals 3(3), 391 (2013) (https://doi.org/10.3390/cryst3030391).
[3] M.V. Yarmolenko, Physics and Chemistry of Solid State 21(2) 294 (2020) (https://doi.org/10.15330/pcss.21.2.294-299).
[4] M.V. Yarmolenko, Mass and Thermal Transport in Engineering Materials, accepted paper, (2020).
[5] S. Kumar, C.A. Handwerker, and M.A. Dayananda, JPEDAV 32, 309 (2011) (10.1007/s11669-011-9907-91547-7037).
[6] K.N. Tu, Electronic Thin-Film Reliability (Cambridge University Press: 2010).
[7] V.V. Morozovych, A.R. Honda, Yu.O. Lyashenko, Ya.D. Korol, O.Yu. Liashenko, C. Cserhati, and A.M. Gusak, Metallofiz. Noveishie Tekhnol. 40(12), 1649 (2018) (10.15407/mfint.40.12.1649).
[8] V.V. Bogdanov, L.N. Paritskaya, and M.V. Yarmolenko, Metallofizika 12(3), 60 (1990).
[9] B. Camin and L. Hansen, Metals 10(8), 1034 (2020) (10.3390/met10081034).
[10] F.J.J. Loo, G.F. Bastin, and J.W.G.A. Vrolijk, Metallurgical and Materials Transactions A 18, 801 (1987) (https://link.springer.com/article/10.1007/BF02646922).
[11] J.E. Morral, Y.-H. Son, M.S. Thompson, Acta Metallurgica 36(8), 1971 (1988) (https://doi.org/10.1016/0001-6160(88)90299-4).
[12] M.V. Yarmolenko, Defect and Diffusion Forum 143-147, 507 (1997) (https://www.scientific.net/DDF.143-147.509).
[13] L.S. Darken, Trans. A.I.M.E. 175, 184 (1948).
[14] Y. Funamizu and K. Watanabe, Transactions of the Japan Institute of Metals 12(3), 147 (1971) (10.2320/matertrans1960.12.147).
[15] A. Gueydan, B. Domenges, and E. Hug, Intermetallics 50, 34 (2014) (DOI: 10.1016/j.intermet.2014.02.007).
[16] F. Moisy, X. Sauvage, E. Hug, Materialia 9, 100633 (2020) (https://doi.org/10.1016/j.mtla.2020.100633).
[17] A. Paul, T. Laurila, V. Vuorinen, S.V. Divinski, Thermodynamics, Diffusion and the Kirkendall Effect in Solids (Springer Cham Heildelberg New York Dordrecht London, 2014) (10.1007/978-3-319-07461-0).
[18] A.M. Gusak and M.V. Yarmolenko, J. Appl. Phys. 73(10), 4881 (1993) (https://doi.org/10.1063/1.353805).
[19] M.V. Yarmolenko, Izvestiya AN SSSR. Metally 3, 182 (1990) (https://publons.com/publon/2915981/).
[20] M.V. Yarmolenko, Deviation from Parabolic Growth of Phase Layers in Cylindrical and Spherical Samples: Curvature and Internal Stress Influence in Proceedings of PTM-1994, W.C. Johnson, J.M. Howe, D.E. Laughlin, and W.A. Soffa (The Minerals, Metals & Materials Society, Pennsylvania, 1994). P.1177 (https://publons.com/publon/3639123/).
[21] M.V. Yarmolenko, Metallofiz. Noveishie Tekhnol. 40(9), 1201 (2018) (10.15407/mfint.40.09.1201).
[22] M.V. Yarmolenko, AIP Advances 8, 095202 (2018) (https://doi.org/10.1063/1.5041728).
[23] M.V. Yarmolenko, A.M. Gusak, and K.P. Gurov, Journal of Engineering Physics and Thermophysics 65, 876 (1993) (https://doi.org/10.1007/BF00862930).

М.В. Ярмоленко

Аналіз відношення внутрішніх коефіцієнтів дифузії у системі Al-Cu

Київський національний університет технологій та дизайну, факультет ринку, інформаційних та інноваційних технологій, Черкаси, Україна, yarmolenko.mv@knutd.edu.ua

Експериментально досліджено електричну корозію міді та алюмінію при кімнатній температурі та при температурі 100 °С. Отримано такий результат: електрична корозія міді значно швидша, ніж електрична корозія алюмінію, але відношення коефіцієнтів корозії, k_{Cu}/k_{Al} , зменшується зі збільшенням температури. Обчислено, що електрична корозія міді та алюмінію приблизно однакова при температурі 300 °С, тому що іони Cu^{2+} менш рухливі, ніж іони Cu^{+}. Фізично це очевидно: з підвищенням температури збільшується амплітуда коливань атомів у кристалічній границі, атоми Cu можуть дифундувати без двох електронів, а взаємодія іонів Cu^{2+} з кристалічною границею значно сильніша, ніж взаємодія іонів Cu^{+}. Для аналізу були використані літературні експериментальні дані.

Ключові слова: мідь; алюміній; електроліз; дифузія; інтерметаліди; кінетика утворення фаз.